Appendix 1

Methods

NGS

For the Next Generation Sequencing (NGS), slides were manually macrodissected, and the RNA was isolated. Library were prepared by the Oncomine Focus Assay (Thermo Fisher Scientific) using a total of 10 ng input RNA per sample. The RNA panel can identify rearrangements in 23 genes including ROS1. Sequencing was performed using the Ion GeneStudio S5 (Thermo Fisher Scientific). Fusions were detected using the fusion detection module within the Ion Reporter workflow, in particular 20,000 was the minimum number of total valid mapped reads required to qualify a sample as valid and to proceed with the analysis.

FISH

The break-apart FISH test is based on a mixture of two probes hybridizing to the proximal (3', green-labeled probe) and distal (5', orange-labeled probe) to the ROS1 breakpoint cluster region. At least 50 non-overlapping tumor nuclei were scored for each specimen by a trained technologist and a pathologist. Cells positive for rearrangement were defined by two main patterns: i) a "split pattern", with 3' and 5' break apart signals at a distance of two times the diameter of the largest signal; ii) a "5' deletion pattern", showing one fusion signal and an isolated 3'green signal (without the corresponding 5' orange signal). A case was considered FISH positive for ROS1 rearrangements when at least 15% of tumor cells showed any split or any 5' deletion pattern.

Whole Transcriptome Sequencing and Whole Exome Sequencing

For Whole Transcriptome Sequencing (WTS), poly(A)-RNA molecules were purified using oligo-dT magnetic beads, then mRNA was fragmented and randomly primed for reverse transcription, followed by second-strand synthesis. The cDNA fragments were end-repaired, ligated using paired-end sequencing adapters and amplified to create the final cDNA library.

For Whole Exome Sequencing (WES), genomic DNA was tagged and fragmented by the Nextera transposon-based technique, then DNA libraries were denatured to single-stranded DNA and hybridized to biotin-labeled 80-mer probes designed to enrich targeted exonic regions, then eluted from magnetic beads and amplified by PCR.

WTS and WES libraries were quality checked and sized with the High Sensitivity kit on the 2100 Bioanalyzer (Agilent Technologies), then quantified using a fluorometric assay (Quant-iT PicoGreen Assay, Life Technologies). Paired-end libraries were sequenced at 2 × 80 bp read length on a Nextseq500 Illumina platform.

NGS data analysis of WES was performed as follows. After cleaning and trimming (https://adapterremoval.readthedocs.io), paired-end reads (80X2) were aligned to human reference HG38 using the Burrows-Wheeler Aligner (http://bio-bwa.sourceforge.net/), bam file manipulation including PCR duplicates removal were performed using Samtools (http://www.htslib.org/). Mapping quality recalibration and local realignment around indels was performed using Genome Analysis Toolkit (GATK4) as well as the detection of single nucleotide variants (SNVs) and indels (function mutect2) (https://gatk.broadinstitute.org). All detected variants were filtered based on quality, coverage >15X, allele ratio >0.2, and the presence in public databases (dbSNP and Exac). Somatic mutations were called by comparing with normal counterpart sample. Functional annotation was performed with Annovar tool (http://www.openbioinformatics.org/annovar/). Differently, WTS data was analyzed with the aim to detect chimeric transcripts adopting a consensus method based on both Chimerascan (https://code.google.com/archive/p/chimerascan/) and Defuse (https://github.com/amcpherson/defuse) algorithms.

Flow Cytometry analysis

PD-L1 detection on ADK-VR2, ADK-VR2 AG143 and HCC-78 was performed by indirect direct immunofluorescence with 5 µg/mL anti-PD-L1 antibody (Tecentriq1200, atezolizumab, Roche). Anti-mouse IgGAF488 (diluted 1:100; Thermo Fisher Scientific) was used as secondary antibody. Cytofluorometric analysis was performed by CyFlow Space (Sysmex Partec, Germany) instrument and analyzed using FCSExpress (De Novo Software, Glendale, CA, USA).

https://dx.doi.org/10.21037/tlcr-22-163

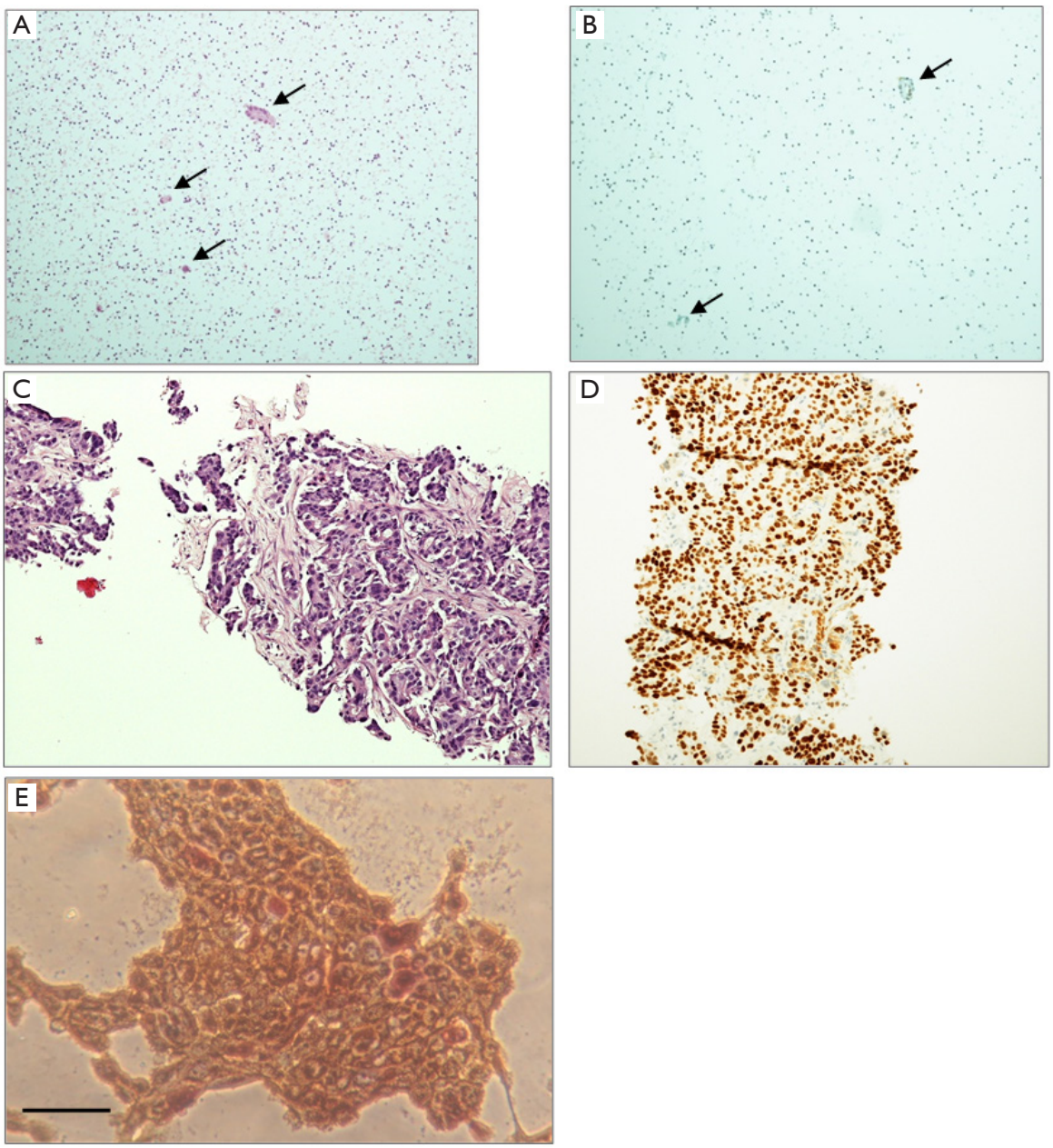

Figure S1 Molecular and morphological characterization of patient's tumor samples and ADK-VR2 cell line. (A,B) Cytological cell blocks from malignant pleural effusion of the patient at the diagnosis. (A) H&E staining showing aggregates of neoplastic cells (arrows) ×10 magnification. (B) TTF1 staining evidencing a focal positivity (arrows) ×10 magnification. (C,D) Liver metastasis. (C) H&E staining. (D) TTF1 staining. (E) BerEP4 staining of ADK-VR2 cell line. Black bar corresponds to 100 µm. H&E, hematoxylin and eosin.

https://dx.doi.org/10.21037/tlcr-22-163

Table S1 Somatic mutations evidenced in ADK-VR2 cells by whole exome sequencing

Gene symbol	NCBI transcript ID	Exon	cDNA variant	Protein variant	Depth of coverage[†]	Allele frequency[‡]
ANK2	NM_001148	exon38	c.C8837A	p.T2946K	220	0.655
CNTNAP5	NM_130773	exon22	c.G3542A	p.R1181H	30	0.367
COX11	NM_001162862	exon1	c.G53T	p.R18L	149	0.517
CSMD1	NM_033225	exon37	c.G5635A	p.A1879T	32	0.625
CWF19L1	NM_001303406	exon4	c.C263T	p.A88V	113	0.239
DEFA6	NM_001926	exon1	c.G130T	p.A44S	89	0.674
DIS3	NM_001128226	exon16	c.C1975G	p.R659G	22	1.000
FGA	NM_000508	exon6	c.G2574A	p.M858I	114	0.377
GNA14	NM_004297	exon1	c.G25A	p.A9T	82	1.000
JKAMP	NM_001284201	exon5	c.A659C	p.Q220P	32	1.000
LOXL2	NM_002318	exon14	c.G2246A	p.G749D	60	0.267
LRP6	NM_002336	exon4	c.A809G	p.D270G	212	0.476
MEI1	NM_152513	exon13	c.G1453A	p.A485T	22	1.000
NUP98	NM_016320	exon29	c.A4492C	p.I1498L	65	1.000
PANX3	NM_052959	exon1	c.G163A	p.A55T	112	0.580
PKD1L1	NM_138295	exon9	c.A1402C	p.S468R	37	0.649
PKHD1	NM_138694	exon41	c.G6698C	p.G2233A	150	0.367
PLB1	NM_001170585	exon57	c.T4219G	p.W1407G	96	0.677
TTC36	NM_001080441	exon3	c.G388A	p.G130R	164	0.396
TTK	NM_001166691	exon17	c.C2044T	p.Q682X	30	0.500
ZBTB24	NM_001164313	exon2	c.G157A	p.A53T	93	0.473
ZNF285	NM_001291489	exon4	c.G809T	p.S270I	159	0.358
DMKN	NM_001190348	exon1	c.G159C	p.K53N	250	0.468

[†], depth of coverage refers to the total number of short reads overlapping the given genomic coordinate in which the mutation was found; [‡], allele frequency refers to the ratio between the number of short reads carrying the mutated allele and the depth of coverage.

Table S2 Drug sensitivity on 2D cultures in ADK-VR2, HCC-78 and clone AG143 to various drugs

Cell line	Pemetrexed (μM)	Crizotinib (μM)	Lorlatinib (μM)	Entrectinib (μM)	DS-6051b (μM)
ADK-VR2	0.0677±0.0130	0.5530±0.0801	>2.5	>1	>1
ADK-VR2 AG143	–	1.5500±0.1463	>2.5	>1	>1
HCC-78	0.0096±0.0009	0.4686±0.2494	<0.01	0.2967±0.1182	0.4309±0.2459

IC_{50} mean ± SEM was reported. SEM, standard error of mean.

Table S3 Drug sensitivity on sphere formation assay in ADK-VR2 and clone AG143 to various drugs

Cell line	Crizotinib (μM)	Lorlatinib (μM)	Entrectinib (μM)	DS-6051b (μM)
ADK-VR2	0.0040±0.0003	0.0003±0.0001	0.0233±0.0049	0.0013±0.0000
ADK-VR2 AG143	0.0236±0.0103	0.0032±0.0012	0.0590±0.0110	0.1060±0.0111

IC_{50} mean ± SEM was reported. SEM, standard error of mean.

https://dx.doi.org/10.21037/tlcr-22-163

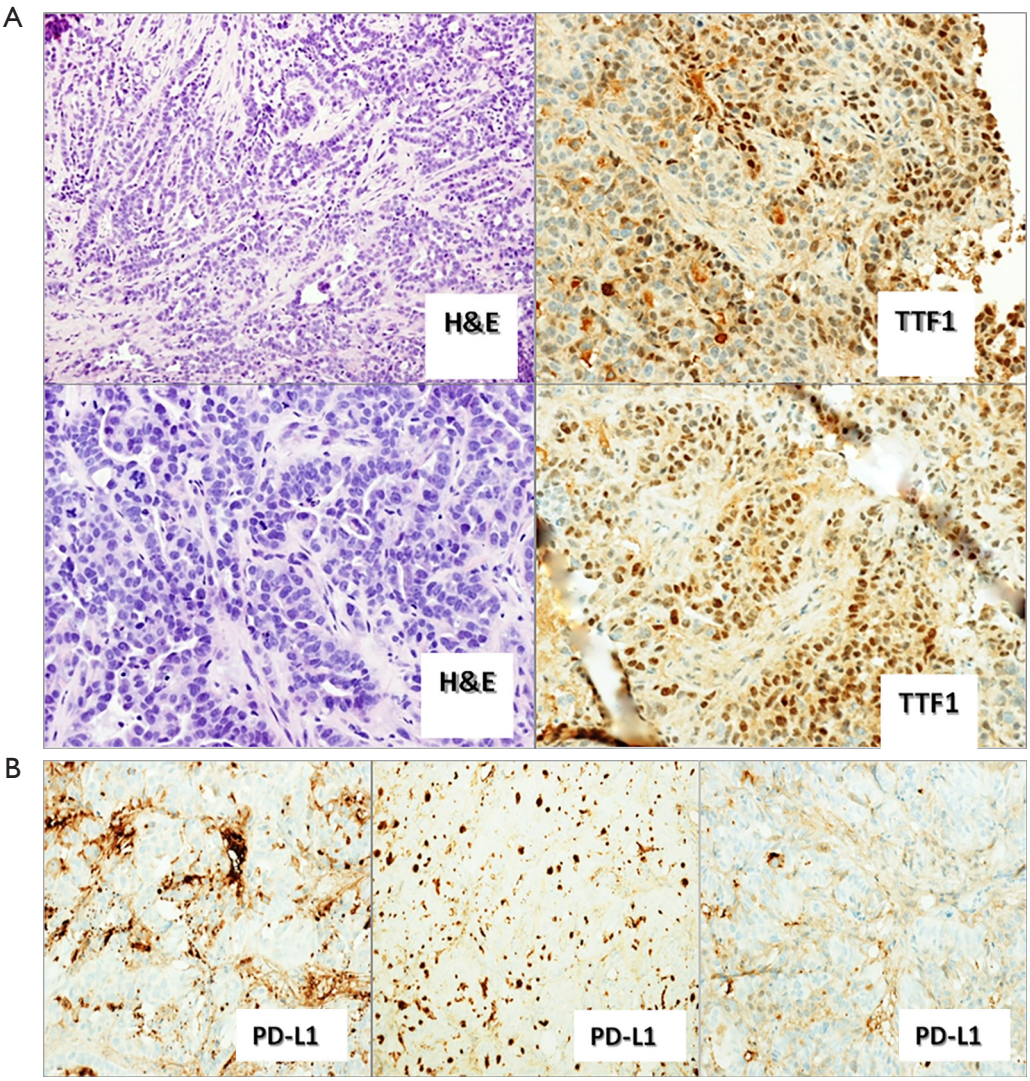

Figure S2 Tumors induced by s.c. injection of ADK-VR2 cells in immunocompromised BRG mice. (A) The phenotype of tumors developed in three different mice was studied. Each row represents a distinct tumor. H&E showed a morphology similar to tumor of patient. TTF1 staining was focal. The third tumor was reported in *Figure 3A* (×10 magnification). (B) PD-L1 staining of three different tumors was weak and focal for the first and second tumor and negative for the third tumor (×10 magnification).

https://dx.doi.org/10.21037/tlcr-22-163

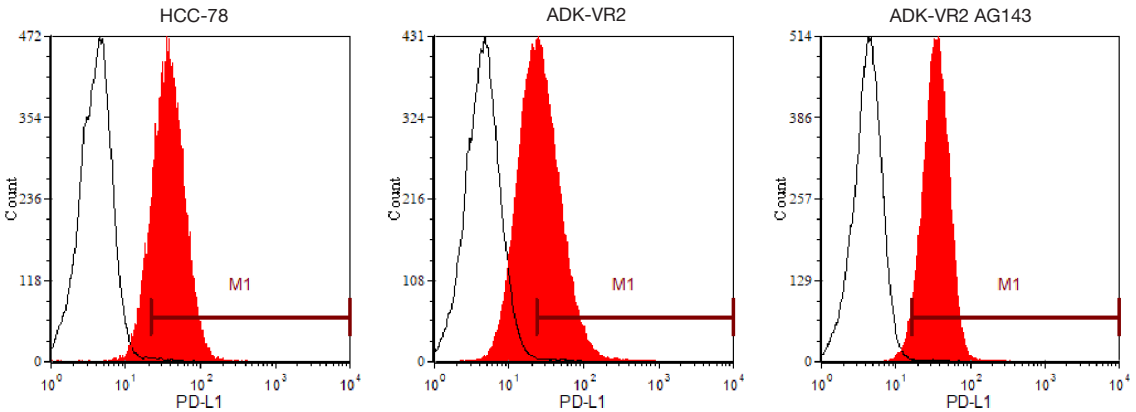

Figure S3 Panels show representative profiles of PD-L1 level expressed on HCC-78, ADK-VR2 and ADK-VR2 AG143 as measured by flow cytometry. Black profile, secondary antibody alone; red profile, anti-PD-L1 antibody.

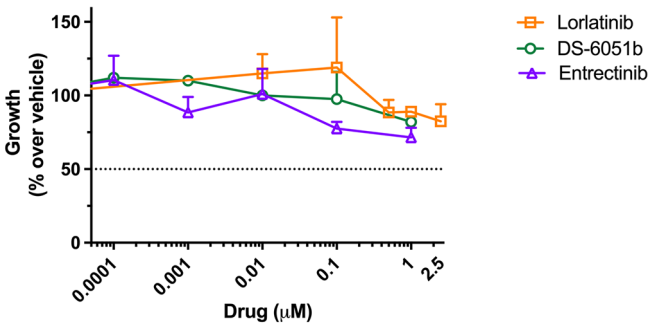

Figure S4 *In vitro* 2D-growth sensitivity of ADK-VR2 AG143 cells to lorlatinib (n=2), DS-6051b (n=2) and entrectinib (n=2). Each point represents mean and SEM. SEM, standard error of mean.

https://dx.doi.org/10.21037/tlcr-22-163

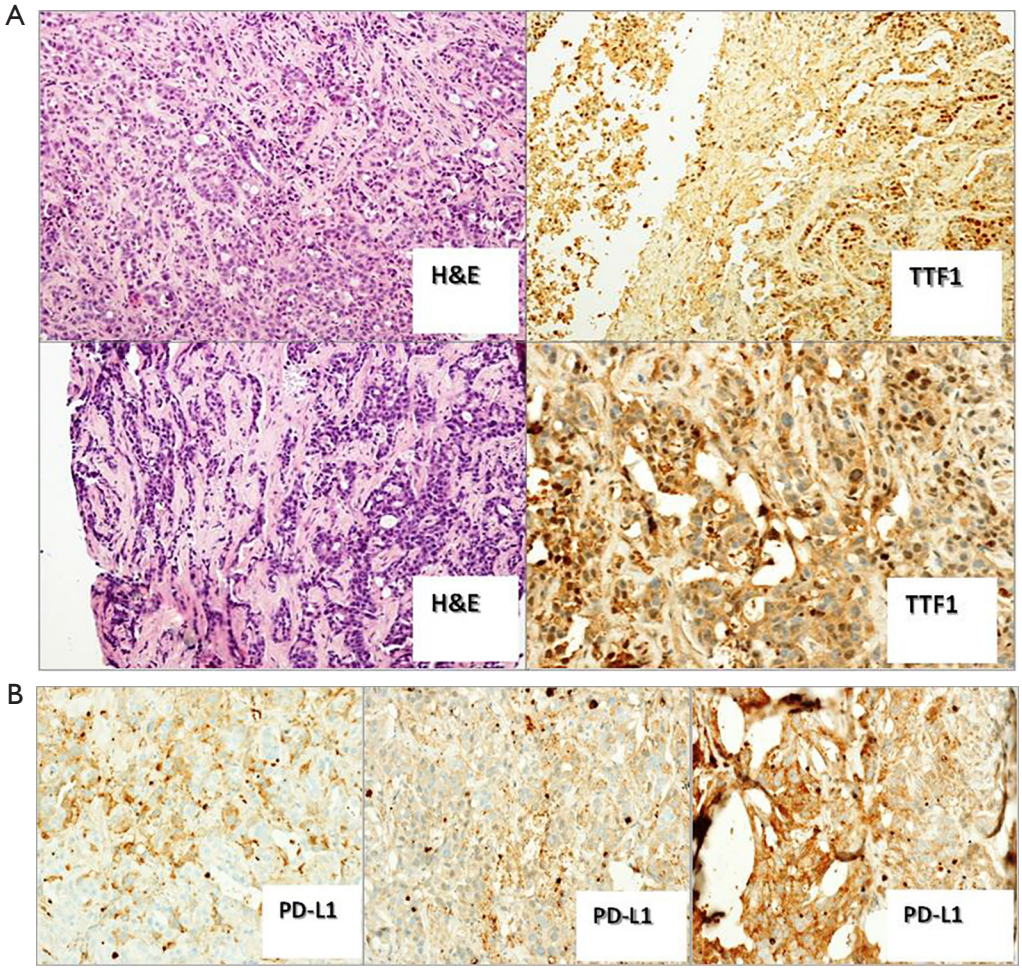

Figure S5 Tumors induced by s.c. injection of ADK-VR2 AG143 cells in immunocompromised BRG mice. (A) The phenotype of tumors developed in three different mice was studied. The picture depicted the tumors of two mice. The third one was included in *Figure 4*. Each row represents a distinct tumor. First column: H&E staining showing a morphology similar to the tumor of the patient. Second column: weak and focal TTF1 staining (×10 magnification). (B) PD-L1 staining of three distinct ADK-VR2 AG143 tumors: the expression was weak and focal for the first and second tumor and negative for the third tumor (×10 magnification). H&E, hematoxylin and eosin.

https://dx.doi.org/10.21037/tlcr-22-163